

## Dipole excitations in open shell nuclides near the neutron threshold energy from $(\gamma, \gamma')$ experiments: The case of Ge isotopes

N. BENOURET<sup>(1)</sup>, R. SCHWENGNER<sup>(2)</sup>, R. MASSARCZYK<sup>(3)</sup>, T. SHIZUMA<sup>(4)</sup>,  
D. BEMMERER<sup>(2)</sup>, R. BEYER<sup>(2)</sup>, A. JUNGHANS<sup>(2)</sup> and A. WAGNER<sup>(2)</sup>

<sup>(1)</sup> Faculty of Physics, University of Sciences and Technology (USTHB) - Algiers, Algeria

<sup>(2)</sup> Helmholtz-Zentrum Dresden-Rossendorf - Dresden, Germany

<sup>(3)</sup> Los Alamos National Laboratory - Los Alamos, NM, USA

<sup>(4)</sup> National Institutes for Quantum and Radiological Science and Technology - Tokai, Ibaraki, Japan

received 31 October 2023

**Summary.** — The dipole response of the open-shell nuclide  $^{70}\text{Ge}$  has been investigated in high-resolution  $(\gamma, \gamma')$  experiments using bremsstrahlung produced with electron beams of energies of 8.5 and 14.7 MeV at the linear accelerator ELBE. A resonance-like structure of levels mostly with spin  $J = 1$  has been identified, distributed between 5 MeV up to neutron separation energy  $S_n$  as in the case of  $^{76}\text{Ge}$  and in contrast to  $^{74}\text{Ge}$  where the level density is lower and ceases abruptly at about 1 MeV below  $S_n$ . The distribution strength was complemented by the unresolved levels using simulations of statistical  $\gamma$ -ray cascades, corrected by estimations of branching transitions. The summed strength in  $^{70}\text{Ge}$ , completed by the data from  $^{74,76}\text{Ge}$  do not fit with a linear trend as function of the neutron excess. Such unexpected behaviour might be related to the nuclear deformation which seems to play the major role in the moderately deformed Germanium isotopic chain.

### 1. – Introduction

The enhancement of dipole strength near the neutron threshold energy, termed as Pygmy Dipole Resonance (PDR) is still the topic of many experimental and theoretical studies. Discovered in neutron shell closure nuclides [1], this extra strength of E1 character, increases significantly reaction rates in the r-process. The PDR excitation was described in most of microscopic approaches as an oscillation of weakly-bound neutron skin against an inert symmetric  $N=Z$  proton-neutron core. The neutron skin thickness seems correlating to the symmetry term of the equation of state which describes neutron stars. Despite its correlation with the neutron excess, the corresponding collectivity is still not clear. To gain more information on PDR properties, we present in this contribution, preliminary results on the open shell stable moderately deformed  $Z=32$   $^{70}\text{Ge}$ , complementing results on  $^{74,76}\text{Ge}$  [2,3] isotopes.

## 2. – Experimental method and results analysis

Two  $^{70}\text{Ge}(\gamma, \gamma')$  experiments were carried out at the bremsstrahlung facility at the superconducting electron accelerator ELBE [7] of the Forschungszentrum HZDR (Dresden-Rossendorf). The bremsstrahlung photon beam was produced by hitting a niobium foil of  $5\ \mu\text{m}$  and  $7\ \mu\text{m}$  with electron beam at kinetic energies of 8.5 MeV and 14.7 MeV, and average currents of 0.7 mA and 0.5 mA, respectively. During the corresponding time of irradiation of about 148 h and 105 h, the generated Bremsstrahlung photon beam was collimated to the investigated target consisting of 508.8 mg of  $^{70}\text{Ge}$  enriched to 97.7% and combined with a disk of 300 mg of Boron enriched to 99.5% in  $^{11}\text{B}$  for the photon flux calibration. The deexciting  $\gamma$  rays were collected by four high-purity germanium (HPGe) detectors surrounded by escape-suppression shields, two mounted at  $127^\circ$  and the other at  $90^\circ$  with respect to the incident photon beam. The absolute detection-efficiency curves of the HPGe detectors were determined by using a  $^{226}\text{Ra}$  standard calibration source up to 2.4 MeV, extrapolated to higher energies using simulations with the GEANT4 code [6]. The absolute photon fluxes in the two measurements were calculated using a bremsstrahlung computer code [4] based on Schiff approximation [5] and then adjusted to the photon flux values obtained from the intensities and known integrated scattering cross sections of transitions in  $^{11}\text{B}$ . An example of deexcitations Spectra of  $^{70}\text{Ge}$  obtained at the two different electron energies are shown in fig. 1(a) by summing the events of spectra at  $127^\circ$ . The spectrum intensity is carried by photons resonantly scattered from  $^{70}\text{Ge}$  forming resolved peaks lying on an exponentially decreasing continuous intensity as a consequence of detector response, unresonantly scattered photons (atomic process) and of the large number of weak unresolved transitions due to the increasing nuclear level density approaching the neutron threshold energy (quasi-continuum) where statistical approaches need to be used to deduce average branching ratios.

**2.1. Resolved strength analysis.** – Due to the low momentum transfer of photons to target nuclei, mainly dipole states and to a lesser extent quadrupole states are photoexcited from the ground state. The comparison of observed transitions in the spectra of two measurements allow to discriminate the inelastic transitions. Transitions observed in the measurements at 8.5 MeV are assumed as ground-state transitions. Additional transitions observed up to 8.5 MeV in the measurements at 14.7 MeV are considered as inelastic transitions from levels at higher excitation energies to low-lying excited states. For the remaining elastic transitions, we checked if sum of the energies of the considered transition and the first excited states ( $2_1^+$ ,  $0_1^+$ ,  $2_2^+$ ) fits the energy of a state at higher excitation energy. In this case it is considered as branching transition (inelastic) and sorted out.

From the intensity of the resolved transitions  $I_\gamma(E_\gamma, \theta)$ , corresponding to the photoexcitation of a state at  $E_x$  excitation energy, the energy and solid angle integrated cross section  $I_s(E_x)$  is deduced as:  $I_s(E_x) = \frac{I_\gamma(E_\gamma, \theta)}{W(E_\gamma, \theta)\Phi_\gamma(E_x)N_N}$  where,  $N_N$  is the number of  $^{70}\text{Ge}$  nuclei in the target,  $\Phi_\gamma(E_x)$  is the photon flux irradiating the target at  $E_x$  and  $W(E_\gamma, \theta)$  is the angular distribution of the considered transition. In order to reduce systematic errors, as the detector live time, the cross sections were calculated relative to the ones known for transitions in  $^{11}\text{B}$ . In NRF experiment, using the measured elastic integrated cross section, the nuclear properties of the excited state as the ground-state width  $\Gamma_0$  can be extracted if the ground-state decay branching ratio  $b_0 = \Gamma_0/\Gamma$  is known, according to :  $I_s(E_x) = \left(\frac{\pi\hbar c}{E_x}\right)^2 \frac{2J_x+1}{2J_0+1} \frac{\Gamma_0^2}{\Gamma}$ , here,  $J_x$  and  $\Gamma$  denote spin and total width of the excited level, respectively, and  $J_0$  is the spin of the ground state. If the decay branching

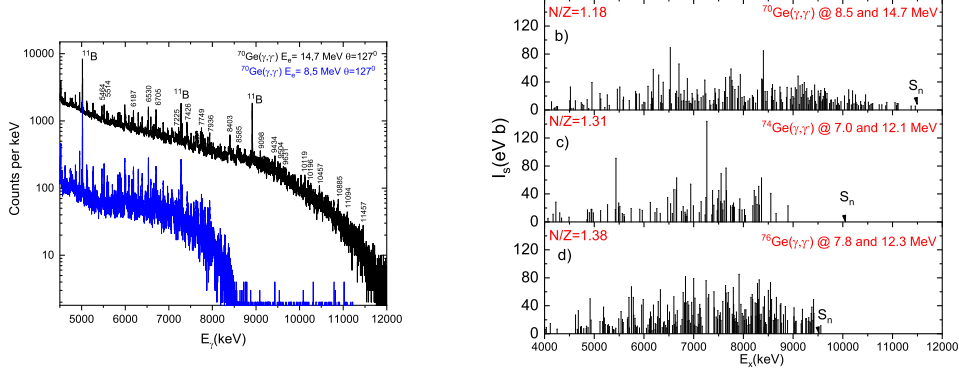


Fig. 1. – (a) NRF Spectra at  $127^\circ$  from  $^{70}\text{Ge}$  combined with  $^{11}\text{B}$  at an electron energy of 8.5 MeV and 14.7 MeV. Elastic scattering cross section distribution results in  $^{70}\text{Ge}$  (b) in comparison to  $^{74,76}\text{Ge}$  (c) [2], (d) [3].

transitions are not observed for a given level,  $b_0$  equal to 1 is assumed. In the case of an electric dipole transition,  $\Gamma_0$  is converted into the electric reduced transition probabilities as:  $B(E1) \uparrow = 9.554 \times 10^{-4} \frac{2J_x + 1}{2J_0 + 1} \frac{\Gamma_0}{E_x^3}$ . Spins of excited states are determined by measuring the angular distribution ratio  $W(90^\circ)/W(127^\circ)$  of the corresponding ground state transition which amounts about 0.74 and 2.28 for a 0-1-0 and 0-2-0 sequence, respectively, taking into account opening angles of the detectors. This ratio is close to unity in case of feeding of the considered level from higher excited states.

In our case, most of the ground-state transitions are clearly dipole transitions thus exciting  $J = 1$  states, a pygmy characteristic.

The measured integrated elastic scattering cross section distribution deduced from all identified ground-state transitions of  $^{70}\text{Ge}$  where the corresponding peak area is above the experimental detection limit are displayed in fig. 1(b), together to the values for the stable isotopes  $^{74,76}\text{Ge}$  (fig. 1(c), (d)) from refs. [3,9]. Note that the strong transition of  $^{70}\text{Ge}$  at 5989 MeV of about 64 eVb known as a magnetic transition [8]; is not considered. In  $^{70}\text{Ge}$ , the enhancement of dipole strength is distributed up to energy threshold as in  $^{76}\text{Ge}$  whereas it ends abruptly in  $^{74}\text{Ge}$  at about 1 MeV below the threshold. The corresponding level density is less fragmented in  $^{74}\text{Ge}$  in comparison to  $^{74,76}\text{Ge}$ . While the dipole strength in  $^{74}\text{Ge}$  seems to be concentrated in two groups of transitions centered around the strongest transitions at 5.5 MeV and 7.2 MeV with an integrated cross section of 91 eVb and 144 eVb, respectively. The dipole strength in  $^{70}\text{Ge}$  seems to be distributed in two groups shifted to higher energy by about 1 MeV. The strength of both groups is similar, it is of about 85 eVb. In the case of  $^{76}\text{Ge}$ , the separation is hardly to distinguish, the strength is more spread, one can separate it in two groups almost not shifted in comparison to  $^{74}\text{Ge}$  at about 5.7 MeV and 7.9 MeV and of about 67 eVb and 87 eVb, respectively. Assuming ground-state transitions ( $b_0 = 1$ ) of electric character, the extracted resolved  $\sum B(E1) \uparrow$  between 5.5 MeV and  $S_n = 11.5$  MeV in  $^{70}\text{Ge}$  is presented in fig. 3, in comparison with those from data of  $^{74,76}\text{Ge}$  from refs. [3,9]. As can be seen, a quite surprising finding in comparison to the usual trend of the PDR strength, corresponding to a linear increase of the resolved summed strength with the neutron excess  $N/Z$  ratio, as found in Sn isotopic chain and in isotopic chain near shell-closures.

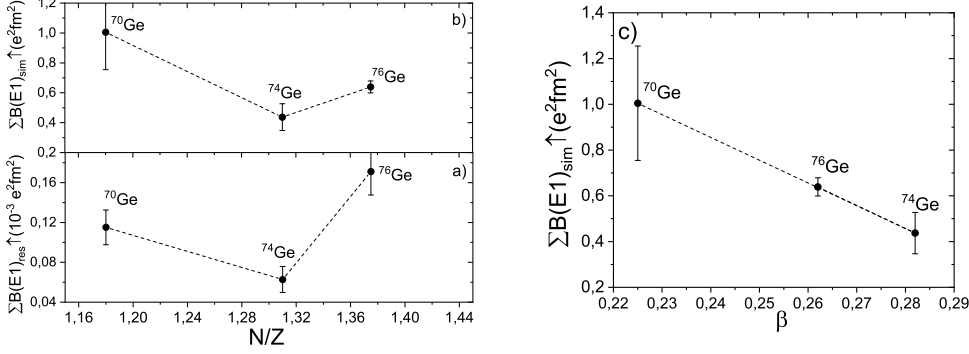


Fig. 2. –  $\sum B(E1) \uparrow$ : (a) resolved, (b) corrected for simulations of branching ratios and quasi-continuum. (c)  $\sum B(E1) \uparrow$  as function of deformation in  $^{70}\text{Ge}$  in comparison to  $^{74,76}\text{Ge}$  [3, 9]

**2.2. Corrected strength analysis.** – In order to correct the intensity of ground-state transitions for their decay branching ratios  $b_0$ , and to account on unresolved levels too (quasi-continuum), we used the  $\gamma$ DEX code for the simulation of statistical  $\gamma$ -ray cascades. The method has been applied already in earlier photon-scattering experiments at  $\gamma$ ELBE [2, 3, 11-13]. The experimental spectra were first unfolded with the detector response and with the non resonant-background using GEANT4. Simulations of 1000 level schemes (nuclear realisations) were carried out. The back-shifted Fermi-gas model was used to estimate the level density. Wigner and Porter-Thomas distribution was applied to account on fluctuations of nearest neighbor spacings and of partial widths of levels, respectively. Considering levels in 0.1 MeV bins in each level scheme, ground state branching ratios  $b_0$  are calculated as the ratio of the sum of intensities of the ground state transitions from all levels in the energy bin to the total intensity of all transitions depopulating those levels to any low-lying levels including the ground state. Using the averaged  $b_0$  over the values of the individual nuclear realizations and the elastic cross section  $\sigma_{\gamma\gamma}(E)$ , the absorption cross section  $\sigma_\gamma$  is derived in each bin:  $\sigma_\gamma(E) = \sigma_{\gamma\gamma}(E)/b_0(E)$ . The absorption cross section  $\sigma_\gamma(E)$  in each bin is transformed to the transition strength  $B(E1) \uparrow (e^2 \text{fm}^2)$  using the relation:  $4.03E_x B(E1) = \sigma_\gamma(E) \Delta E_x$  where the  $\Delta E_x$  is the bin energy.

The summed reduced transition strengths  $\sum B(E1) \uparrow$  corrected for the ground-state branching ratio (simulated) in the energy range 5.5 MeV to  $S_n = 11.5$  MeV for  $^{70}\text{Ge}$  is shown in fig. 2(a). in comparison to those in  $^{74,76}\text{Ge}$  in the same energy range from refs. [3, 9]. Including the correction of the branching ratios on the summed Strength, the trend remains roughly the same, a drop of the strength in  $^{74}\text{Ge}$ . The small difference between the resolved summed strength in  $^{74,76}\text{Ge}$  in comparison to the case accounting on the branching ratio could be due to the overestimation of the branching ratio value in  $^{76}\text{Ge}$ . One possible explanation of this behaviour is connected to the effect of the quadrupole deformation which seems playing the major role in the isotopic chain  $^{70,74,76}\text{Ge}$  in comparison to the neutron excess as it is shown in fig. 2(b). Such behaviour has been pointed out by [9] in the case of heavier Xenon isotopes. Thus, in the case of Germanium chain, the excitation of neutrons might be inhibited by the deformation, manifested by the scarcity of  $J = 1$  states in  $^{74}\text{Ge}$  in comparison to  $^{74,76}\text{Ge}$ , approaching the threshold energy. Above the threshold, the main intensity goes into the  $(\gamma, n)$  channel

and  $(\gamma, \gamma')$  becomes very small and the NRF technique cannot test whether part of this has PDR character. Usually, the  $(\gamma, n)$  cross section is considered as GDR character.

However, the systematic theoretical studies by [10] of the PDR fraction in the nuclear chart as function of the neutron number reported a drop of the PDR strength in  $^{72}\text{Ge}$  instead of  $^{74}\text{Ge}$ . Therefore, further investigations on  $^{72}\text{Ge}$  isotope are needed.

## REFERENCES

- [1] SAVRAN D. *et al.*, *Prog. Part. Nucl. Phys.*, **70** (2013) 210.
- [2] MASSARCZYK R. *et al.*, *Phys. Rev. C*, **92** (2015) 044309.
- [3] SCHWENGER R. *et al.*, *Phys. Rev. C*, **105** (2022) 024303.
- [4] HAUG E. *et al.*, *Radiat. Phys. Chem.*, **77** (2008) 207.
- [5] SCHIFF L. I. *et al.*, *Phys. Rev.*, **83** (1951) 252.
- [6] ALLISON J. *et al.*, *Nucl. Instrum. Methods. Phys. Res. A*, **835** (2016) 186.
- [7] SCHWENGER R. *et al.*, *Nucl. Instrum. Methods A*, **555** (2005) 211.
- [8] JUNG A. *et al.*, *Nucl. Phys. A*, **584** (1995) 103.
- [9] MASSARCZYK R. *et al.*, *Phys. Rev. Lett.*, **112** (2014) 072501.
- [10] EBATA S. *et al.*, *Phys. Rev. C*, **90** (2014) 024303.
- [11] SCHWENGER R. *et al.*, *Phys. Rev. C*, **76** (2007) 034321.
- [12] RUSEV G. *et al.*, *Phys. Rev. C*, **77** (2008) 064321.
- [13] BENOURET N. *et al.*, *Phys. Rev. C*, **79** (2009) 014303.